ACS APPLIED MATERIALS & INTERFACES

Letter

www.acsami.org

pH-Controlled Selective Etching of Al_2O_3 over ZnO

Kaige G. Sun,*[,†,‡] Yuanyuan V. Li,[†,‡] David B. Saint John,[†,§] and Thomas N. Jackson[†,‡]

[†]Center for Thin Film Devices and Materials Research Institute, [‡]Department of Electrical Engineering, and [§]Department of Material Science Engineering, Penn State University, University Park, Pennsylvania 16802, United States

ABSTRACT: We describe pH-controlled selective etching of atomic layer deposition (ALD) Al_2O_3 over ZnO. Film thickness as a function of etch exposure was measured by spectroscopic ellipsometry. We find that alkaline aqueous solutions with pH between about 9 and 12 will etch Al_2O_3 at useful rate with minimal attack of ZnO. Highly selective etching of Al_2O_3 over ZnO (selectivity >400:1) and an Al_2O_3 etch rate of ∼50 nm/min can be obtained using a pH 12 etch solution at 60 °C.

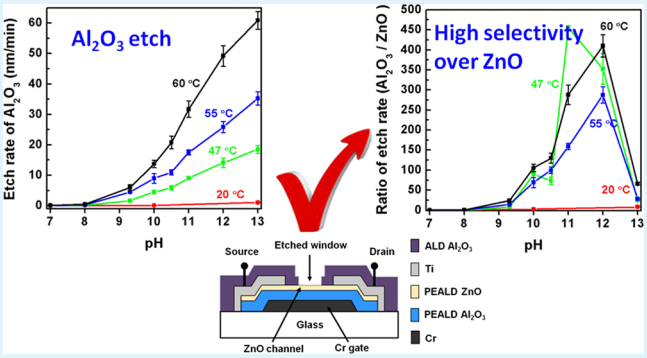

KEYWORDS: *selective etching, zinc oxide, ZnO, aluminum oxide, Al_2O_3, thin film transistor, TFT, metal oxide semiconductor, metal oxide thin film transistors, metal oxide gas sensor, InGaZnO, GaInZnO*

Al_2O_3 is widely used as a high-*k* gate dielectric and passivation material in the fabrication of ZnO thin film transistors (TFT)[1−4] and for other ZnO device structures such as light-emitting diodes,[5] chemical sensors,[6] and surface acoustic wave biosensors.[7] For many applications, it would be useful to etch Al_2O_3 selectively with respect to ZnO.

We have previously reported ZnO TFTs with atomic layer deposition (ALD) Al_2O_3 as passivation layer.[8] A selective etch for Al_2O_3 would allow contact windows to be opened for contacts after passivation or windows in the passivation layer to be opened for sensors. However, Al_2O_3, deposited with ALD or plasma enhanced atomic layer deposition (PEALD) is robust and is commonly wet etched in strong acids such as phosphoric or hydrofluoric acid.[9] Both of these attack ZnO and have etch rates for ZnO much larger than for Al_2O_3.

In this paper, pH-controlled selective etching of ALD Al_2O_3 over ZnO is described. The Al_2O_3 and ZnO thin films used in this work were deposited on oxidized silicon wafers by ALD or PEALD at 200 °C. Films used for etch rate measurements were typically 30 nm thick for Al_2O_3 and 60 nm thick for ZnO. To facilitate etch rate measurements, we developed a parameterized optical model with bulk and surface roughness layers for our ZnO and Al_2O_3 from measurements of as-deposited samples with a J.A.Woollam RC2 VASE spectroscopic ellipsometer with a spectral range of 0.7−5.15 eV at four angles of incidence (50, 60, 70, 80°). The surface roughness layer was modeled by a Bruggeman effective medium approximation (EMA) with 50% void and 50% underlying material. For etch rate measurements, the fitted thickness included the bulk film thickness and half of the surface roughness layer thickness. During the etching experiments, the films before and after etching were measured using a J.A.Woollam M-2000 V spectroscopic ellipsometer with a spectral range of 1.24−3.34 eV at a single angle of incidence (75°). Only the bulk film and surface roughness thicknesses were allowed to vary, whereas the parameterized optical model was fixed to that determined using the wider spectral range and multiple incident angles.

The measurements of etch rate at different pH conditions were done for solutions with pH ranging from 7 to 13. Tetramethylammonium hydroxide (TMAH) and water were the main components for the solutions with high hydroxide ion concentration (pH 12 to pH 13). For pH from 7 to 11, sodium phosphate (Na_3PO_4), monopotassium phosphate (KH_2PO_4), sodium carbonate (Na_2CO_3) and sodium bicarbonate ($NaHCO_3$) were added to the solutions as buffers to stabilize the pH during etching. The total amount of the buffer used was controlled to keep the anion concentration around 0.1 mol/L.

Figure 1 shows the measured etch rate of Al_2O_3 as a function of pH for etch temperatures of 20, 47, 55, and 60 °C. As shown in Figure 1, the etch rate of Al_2O_3 increases with both pH and temperature. The measured etch rate of ZnO in the range from pH 9 to pH 12 is less than 0.4 nm/min and changes little with temperature. Examination of the two-layer ellipsometry fitting results indicates that the small apparent ZnO etch rate in the pH 9 to pH 12 range is mainly caused by increasing ZnO surface roughness.

Figure 2 shows the etch selectivity for Al_2O_3 with respect to ZnO as a function of pH for etch temperatures of 20, 47, 55, and 60 °C. At 20 °C the ratio of Al_2O_3 to ZnO etch rate is less than 10. Because the Al_2O_3 etch rate is strongly temperature activated while the ZnO etch rate changes little with

Received: March 28, 2014
Accepted: May 12, 2014
Published: May 12, 2014

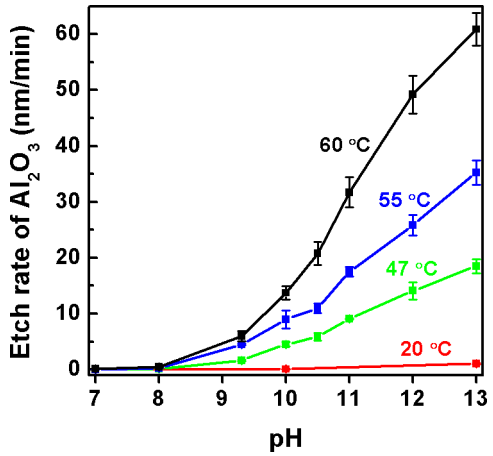

Figure 1. Etch rate of Al_2O_3 versus pH for etch temperatures of 20, 47, 55, and 60 °C. For pH >8, the etch rate increases rapidly with pH and temperature.

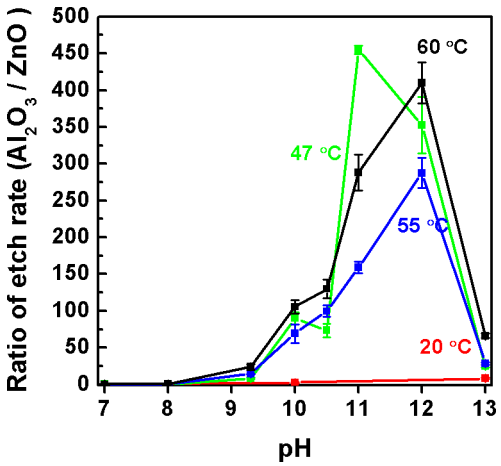

Figure 2. Etch selectivity for Al_2O_3 with respect to ZnO versus pH for etch temperatures of 20, 47, 55, and 60 °C. Because the etch rate for ZnO is very small and approximately independent of temperature for 9 < pH ≤ 12, the etch selectivity at elevated temperature is large in this range.

temperature, the etch rate ratio of Al_2O_3 to ZnO increases with increasing temperature. For a pH 12 etch solution at 60°C the ratio of the Al_2O_3 to ZnO etch rate is larger than 400 (49.2 ± 3.4 nm/min over 0.12 ± 0.04 nm/min). The error bars shown in Figure 2 are for the ellipsometry measurement of the Al_2O_3 etching and the etch rate ratio was found using the mean of four ZnO etch tests at each pH and temperature. As pH and temperature are increased the etch rate for Al_2O_3 increases and it becomes more difficult to precisely determine etch selectivity using our technologically relevant thin films. The data in Figure 2 shows the trends, but the detailed ordering of etch selectivity with temperature for 11 ≲ pH ≲ 12, where the etchant is most selective, is less certain.

To confirm that the selective etching is pH-based, we also characterized an etch solution using 0.25 mol/L sodium hydroxide (NaOH). The pH of the solution was set to 10.5 using a Na_2CO_3/$NaHCO_3$ pH 10 buffer commercially available as Hydrion® buffer. The etch rates of Al_2O_3 and ZnO at 60°C in the NaOH-based etchant were 19.2 ± 2.1 nm/min and 0.16 ± 0.06 nm/min, similar to that of the TMAH-based etchant (Al_2O_3 20.8 ± 2.1 nm/min and ZnO 0.16 ± 0.03 nm/min), which supports the conclusion that hydroxide ions are responsible for Al_2O_3 etching. Although the selective etch is pH-based, some care is required in choosing the alkaline agent. For example, ammonium hydroxide (NH_4OH) is a convenient base. But ammonium hydroxide is able to chelate ZnO and the etch selectivity for NH_4OH-based etch solutions is reduced compared to TMAH-based or NaOH-based etch solutions.

The reaction between Al_2O_3 and hydroxide ions is

$$Al_2O_3 + 2OH^- \rightarrow 2AlO_2^- + H_2O \quad (1)$$

This is a heterogeneous reaction between a solid phase and ions in a liquid phase. The main factors influencing reaction rate are hydroxide ion concentration, bond energy of the Al−O bonds, and temperature. The rate equation is

$$\text{rate} = k[OH^-]^n = k10^{(pH-14)n} = k\exp((\ln 10)(pH - 14)n) \quad (2)$$

where k is the rate coefficient and n is the order of the reaction.[10] For this simple model, the etch rate of Al_2O_3 should increase exponentially with increasing pH value. Accordingly, an exponential function in the form of $y = A + B^*\exp(C^*x)$ was used to fit the curves of the etch rates at each temperature. The resulting equations and curves are shown in Figure 3. In

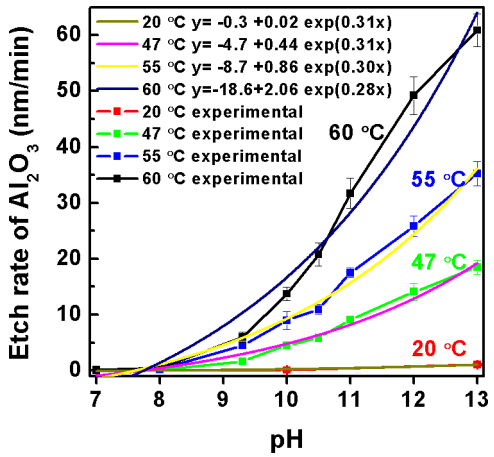

Figure 3. Exponential fitting equations and curves for the data of Figure 1 for etch rates of Al_2O_3 versus pH at temperature 20, 47, 55, and 60 °C.

Table 1. Rate Equations and Extracted Parameters

temp (°C)	reformed equation	n	k
20	rate = 1.82 × $[OH^-]^{0.135}$ − 0.297	0.135	1.82
47	rate = 32.9 × $[OH^-]^{0.134}$ − 4.722	0.134	32.9
55	rate = 60.8 × $[OH^-]^{0.132}$ − 8.725	0.132	60.8
60	rate = 108.7 × $[OH^-]^{0.123}$ − 18.57	0.123	108.7

Table 1, the rate equations are expressed as a function of OH ion concentration and the characteristic parameters are extracted. The rate coefficient k is a function of temperature and the relationship is given by an Arrhenius equation[10]

$$k(T) = A\exp\left(-\frac{E_a}{RT}\right) \quad (3)$$

dx.doi.org/10.1021/am501912q | ACS Appl. Mater. Interfaces 2014, 6, 7028−7031

where A is the pre-exponential factor, E_a is the activation energy, and R is the ideal gas constant. Fitting the rate coefficient k as a function of temperature the activation energy E_a is calculated to be 8.0×10^4 J/mol.

To provide a simple unified rate equation for the selective etch, we also used Eureqa from the Cornell Creative Machine Lab[11] to fit our etch data. Using this tool gives a heuristic rate equation

$$\text{rate} = 3.56 \times 10^{14} \exp\left(-\frac{9609}{T}\right)([OH^-]^{0.139} - 0.143) \quad (4)$$

The activation energy E_a in this rate equation is 0.83 eV/ion or 8.0 x 10^4 J/mol, consistent with the result from the fitting of individual curves.

To apply the selective etch to device fabrication, we have tested compatibility with photoresist. We find DNQ-Novolac photoresist (e.g. Shipley 1811) and poly(methyl methacrylate) (PMMA) can withstand etching solutions of pH 10 to 12 at 60 °C for more than 10 min. Because DNQ-Novolac is also developed in alkaline solutions there may be some change in feature size, particularly for higher pH selective etching. We did not characterize this effect.

For etching device structures, we typically make two additions to our etchant. First, we add a small concentration of a surfactant (3,5-dimethylhexyne-3-ol, commercially available as Surfynol®-6L) to improve the uniformity of etching for small features. We also add a small amount of ZnO to the etch solution to stabilize the initial etch condition. Our etch testing has not shown this to be necessary, but it has been suggested that this can help supply an equilibrium concentration of ions of the non-etching material.[12] The etch rate of the modified etchant is unchanged from that of the etchant without surfactant or ZnO.

We have used the pH-controlled etchant to fabricate tri-layer PEALD ZnO TFTs with selective etching of Al_2O_3 used to open source and drain contact windows.[13] However, this is not a conclusive demonstration of the selective etch because it is possible that the etchant might attack the ZnO, but still allow contacts to work. To better demonstrate the selective etch, we used it to etch windows through the passivation layer in the channel region of TFTs with 10 nm thick ZnO active layers and then re-passivated the devices. Because the passivation step introduces charge at the ZnO/Al_2O_3 interface,[3] this test is sensitive to small changes in the ZnO thickness.

The bottom-gate TFT process used for the selective etch test has been described previously.[8] The TFTs used 10 nm thick ZnO active layers and the passivation layer was 30 nm thick Al_2O_3 deposited by ALD. The TFTs fabricated for this work had mobility >17 $cm^2\ V^{-1}\ s^{-1}$, current on−off ratio >1 × 10^7, and turn-on voltage (here defined as the gate voltage where the linear region drain current reaches 1 × 10^{-10} A) approximately −3.2 V. The negative turn-on voltage was caused by passivation-induced charge.[3]

To demonstrate the selective etch, we used the etchant described above with pH 12 at 47 °C to etch windows in the passivation layer of the bottom-gate TFTs. This etchant temperature was chosen because it gives a convenient and controllable etching time for the passivation layer. The structure after window etching is shown in Figure 4a. After etching windows, we confirmed access to the ZnO channel layer by exposing test TFTs to a few ppm concentration of ozone and observing large changes in current-voltage characteristics. After selective etching, we then deposited 30 nm of Al_2O_3 to re-passivate the window areas.

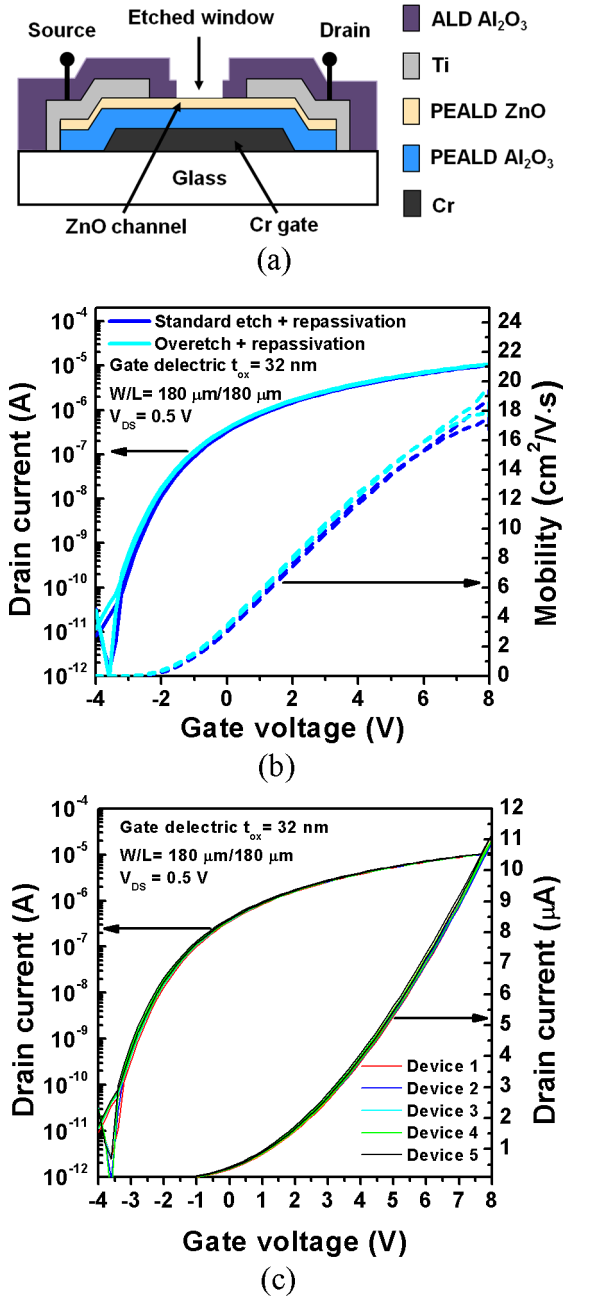

Figure 4. (a) Structure of etch test device. (b) Log(I_D) and mobility versus V_{GS} for V_{DS} = 0.5 V of re-passivated device with standard etch and overetch. (c) Log(I_D) and I_D versus V_{GS} for V_{DS} = 0.5 V of multiple overetched devices after re-passivation.

Figure 4b shows the log of the drain current and differential mobility versus gate voltage for etched and re-passivated TFTs in the linear region of operation. Characteristics are shown for TFTs with the first ALD Al_2O_3 passivation layer etched for the nominal time required to reach the ZnO channel (150 s), and for TFTs etched for twice the nominal time (300 s).

Clearly, the thin ZnO channel remained even for TFTs with overetched channel region windows and the TFT characteristics for both etch times are very similar. Figure 4c shows the linear region log and linear drain current versus gate voltage for five TFTs with overetched (twice nominal etch time) windows.

dx.doi.org/10.1021/am501912q | ACS Appl. Mater. Interfaces 2014, 6, 7028−7031

Although the substrate size used for this test was small (about 1.7 cm × 1.7 cm) the uniformity is quite good. As noted earlier, we have also used the pH-controlled etchant to fabricate tri-layer PEALD ZnO TFTs with selective etching of Al_2O_3 used before source and drain contact deposition.[13] The bias stress stability of the tri-layer TFTs fabricated using the selective etch is equal to or better than that of our non-selective-etch TFTs.

We have described a highly selective pH-controlled etch for Al_2O_3 over ZnO. The etching is simple, easily controlled, and provides highly selective etching. Using TMAH and suitable pH-buffers at $10 \lesssim pH \lesssim 12$ and $40\ ^\circ C < T < 80\ ^\circ C$ provides useful etch rates and high selectivity (>50/1). This allows Al_2O_3 films to be etched even over very thin ZnO layers for use in thin film transistors, metal oxide gas sensors, and optical devices. Preliminary results show similar etch selectivity for similar metal oxide semiconductors, including InGaZnO. This selective etch is a flexible tool for oxide semiconductor device fabrication.

AUTHOR INFORMATION

Corresponding Author

*E-mail: kus194@psu.edu.

Notes

The authors declare no competing financial interest.

ACKNOWLEDGMENTS

This work was supported by Dow Chemical Company and National Science Foundation (NSF) Nanosystems Engineering Research Center (ERC) on Advanced Self-Powered Systems of Integrated Sensor Technologies (EEC-1160483).

REFERENCES

(1) Kawamura, Y.; Horita, M.; Ishikawa, Y.; Uraoka, Y. Effects of Gate Insulator on Thin-Film Transistors With ZnO Channel Layer Deposited by Plasma-Assisted Atomic Layer Deposition. *J. Dispersion Technol.* **2013**, *9* (9), 694−698.

(2) Yang, J.; Park, J. K.; Kim, S.; Choi, W.; Lee, S.; Kim, H. Atomic-layer-deposited ZnO Thin-Film Transistors with Various Gate Dielectrics. *Phys. Status Solidi A* **2012**, *209* (10), 2087−2090.

(3) Mourey, D. A.; Burberry, M. S.; Zhao, D. A.; Li, Y. V.; Nelson, S. F.; Tutt, L.; Pawlik, T. D.; Levy, D. H.; Jackson, T. N. Passivation of ZnO TFTs. *J. Soc. Inf. Disp.* **2010**, *18* (10), 753−761.

(4) Shinhyuk, Y.; Doo-Hee, C.; Min Ki, R.; Sang-Hee Ko, P.; Chi-Sun, H.; Jin, J.; Jae Kyeong, J. High-Performance Al-Sn-Zn-In-O Thin-Film Transistors: Impact of Passivation Layer on Device Stability. *IEEE Electron Device Lett.* **2010**, *31* (2), 144−146.

(5) Wang, T.; Wu, H.; Zheng, H.; Wang, J. B.; Wang, Z.; Chen, C.; Xu, Y.; Liu, C. Nonpolar Light Emitting Diodes of m-Plane ZnO on c-Plane GaN with the Al2O3 Interlayer. *Appl. Phys. Lett.* **2013**, *102* (14), -.

(6) Gieraltowska, S.; Wachnicki, L.; Witkowski, B. S.; Guziewicz, E.; Godlewski, M. Thin Films of High-k Oxides and ZnO for Transparent Electronic Devices. *Chem. Vap. Deposition* **2013**, *19* (4-6), 213−220.

(7) Kim, Y. W.; Sardari, S. E.; Meyer, M. T.; Iliadis, A. A.; Wu, H. C.; Bentley, W. E.; Ghodssi, R. An ALD Aluminum Oxide Passivated Surface Acoustic Wave Sensor for Early Biofilm Detection. *Sens. Actuators, B* **2012**, *163* (1), 136−145.

(8) Mourey, D. A.; Zhao, D. A.; Sun, J.; Jackson, T. N. Fast PEALD ZnO Thin-Film Transistor Circuits. *IEEE Trans. Electron Devices* **2010**, *57* (2), 530−534.

(9) Davidovic, D.; Tinkham, M. Coulomb Blockade and Discrete Energy Levels in Au Nanoparticles. *Appl. Phys. Lett.* **1998**, *73* (26), 3959−3961.

(10) Connors, K. A. *Chemical Kinetics: The Study of Reaction Rates in Solution*, 1st ed.; VCH: New York, 1990; p 10.

(11) Schmidt, M.; Lipson, H. Distilling Free-Form Natural Laws from Experimental Data. *Science* **2009**, *324* (5923), 81−85.

(12) Beverskog, B.; Puigdomenech, I. Revised Pourbaix Diagrams for Zinc at 25−300 °C. *Corros. Sci.* **1997**, *39* (1), 107−114.

(13) Li, Y. V.; Sun, K. G.; Ramirez, J. I.; Jackson, T. N. Trilayer ZnO Thin-Film Transistors With *In Situ* Al_2O_3 Passivation. *IEEE Electron Device Lett.* **2013**, *34* (11), 1400−1402.